

# The Least-Squares Calibration on the Micro-Arcsecond Metrology test bed

Chengxing Zhai, Mark Milman, and Martin Regehr  
Jet Propulsion Laboratory,  
California Institute of Technology,  
Pasadena, CA, 91109

April 12, 2006

## Abstract

The Space Interferometry Mission(SIM) will measure optical path differences (OPDs) with an accuracy of tens of picometers, requiring precise calibration of the instrument. In this article, we present a calibration approach based on fitting star light interference fringes in the interferometer using a least-squares algorithm. The algorithm is first analyzed for the case of a monochromatic light source with a monochromatic fringe model. Using fringe data measured on the Micro-Arcsecond Metrology(MAM) testbed with a laser source, the error in the determination of the wavelength is shown to be less than 10pm. By using a quasi-monochromatic fringe model, the algorithm can be extended to the case of a white light source with a narrow detection bandwidth. In SIM, because of the finite bandwidth of each CCD pixel, the effect of the fringe envelope can not be neglected, especially for the larger optical path difference range favored for the wavelength calibration. We eliminate the fringe envelope effect by “projecting away” the fringe envelope, *i.e.* working in a subspace orthogonal to the envelope signal. The resulting fringe envelope parameters are needed for subsequent OPD estimation in SIM. We show the sensitivities to various errors. The algorithm is validated by using both simulation and the fringe data obtained on the MAM test bed.

## 1 Introduction

The Space Interferometry Mission(SIM) will dither the optical path difference (OPD), and then estimate the OPD from the observed fringes using an estimation algorithm. In order to form an accurate estimate, it is necessary to have the correct fringe model parameters. The fringe model for a monochromatic light source (a laser source, for

example) is characterized by four parameters, namely the intensity, visibility, wave number, and phase dispersion. The conventional OPD estimation algorithm estimates the delay by fitting the fringes to a cosine curve[3]; this requires knowledge of the wavelength of the light source. We shall describe a least-squares calibration scheme suitable for determining the wavelength to high accuracy. We applied this algorithm to the FAM (full aperture metrology) laser interference fringe data obtained on MAM test bed and found that the calibrated wavelength is accurate to 10pm.

The least-squares calibration algorithm can also determine the phase dispersion, intensity and visibility of the fringe signal. This is useful for SIM. For SIM, star light serves as the light source for the interferometers. In the limit of small optical bandwidth, e.g., at the CCD pixel detection bandwidth level, the fringe pattern may be approximated as monochromatic to the leading order. Using the least-squares calibration enables us to obtain all the model parameters at the pixel level. To reduce the effect of read noise, SIM reads groups of CCD pixels simultaneously. A broadband signal may be modeled as a superposition of the pixel-level quasi-monochromatic signals. By performing the least-squares calibration at the pixel level we are able to obtain the effective intensity, visibility, wave number, and the dispersion phase, which form the principal model parameters for the interferometer.

For high precision measurements, we require accurate calibrations. At the accuracy of picometer level required for SIM[1], the fringe envelope for even the narrow optical bandwidth of a CCD pixel is not negligible. Ignoring the envelope may lead to tens of picometers of error in phase calibration and more than 5% error in the visibility. In order to take the fringe envelope into account, we shall first model the leading order fringe envelope using a quadratic function. The fringe envelope effect is then eliminated by working in a subspace that is orthogonal to the envelope factor. The fringe envelope is essentially projected away, removing the systematic error otherwise present in a monochromatic model. The cost of this approach is some increase in the error in the estimates of the other parameters, especially the visibility and the wave number. Once we have the wave number and phase, it is possible to estimate the width and center of the fringe envelope. The envelope width can be used in a broadband delay estimation algorithm.[2] The technique of projecting away the envelope effect is first demonstrated using simulated fringes to validate the idea. We then apply it to white light fringe data from the MAM test bed.

## 2 The least-squares calibration for a monochromatic light source

In this section, we summarize the least-squares calibration algorithm based on a monochromatic fringe model[4].

Given a set of fringe measurements  $y_i$  and the corresponding dithering step posi-

tions  $u_i$ , we seek the wavelength of the light source. Using a least-squares fit to the fringe measurements with a monochromatic model we obtain the wavelength, and also the intensity, visibility, and the phase offset. A monochromatic model may be written as

$$y_i = I [1 + V \cos(ku_i + \phi)], i = 1, 2, \dots, N \quad (1)$$

where  $I$ ,  $V$ ,  $k$ , and  $\phi$  are the intensity, visibility, wave number, and the an offset phase respectively.<sup>1</sup> This may be conveniently expressed as a vector equation

$$y = A(k)x, \quad (2)$$

where  $x \equiv [I \quad IV \cos(kd) \quad IV \sin(kd)]^T$  is the phasor and matrix  $A(k, u)$  is defined by

$$A(k) = \begin{pmatrix} 1 & \cos(ku_1) & -\sin(ku_1) \\ 1 & \cos(ku_2) & -\sin(ku_2) \\ \vdots & \vdots & \vdots \\ 1 & \cos(ku_N) & -\sin(ku_N) \end{pmatrix}.$$

It is useful to view Eq. (2) as a transform from phasor  $x$  to the fringe  $y$ . The column vectors of  $A(k)$  are the basis vectors spanning the model signal space, and the signal  $y$  is a linear combination of these vectors, with coefficients given by the elements of the phasor  $x$ . The minimization question (i.e., the least-squares fit) may be formulated as

$$\min_{k,x} |y - A(k)x|^2 \quad (3)$$

to find the optimal  $k$  and  $x$ . For a given  $k$ , we know that the best  $x$  is given by

$$x(k) = A(k)^\dagger y, \quad (4)$$

where  $A(k)^\dagger$  is the pseudoinverse of the matrix  $A(k)$ . Therefore, the minimization problem may be reduced to a one-dimensional question as

$$\min_k |y - A(k)A(k)^\dagger y|^2. \quad (5)$$

Note that  $A(k)A(k)^\dagger$  is a projection operator to  $A(k)$ 's range space. Thus, the optimization process is really the search for the  $k$  for which the range space of  $A(k)$  has maximal overlap with the signal  $y$ , i.e., for which the projection of  $y$  in the range space of  $A(k)$  is maximized. A QR-factorization can be conveniently used here to find the range space of  $A(k)$  as  $Q(k)R(k) = A(k)$ . The minimization problem may be expressed simply as finding the  $k$  that maximize the projection  $|Q(k)y|$ . We note that not only can we obtain the wave number, we are able to also find the corresponding intensity, visibility, and the phase offset by using relation (4) for the optimal wave number.

---

<sup>1</sup>Here we have assumed a staircase dither waveform. For a continuous triangle dither, the only difference is a "sinc" factor.

### 3 Sensitivity to signal error

Before we consider the case where the fringe model deviates from the nominal monochromatic model, it is useful to study the sensitivity of the calibration scheme described above. Consider the relation between the variation of the parameters and the corresponding signal

$$\delta y_i = \delta I + (\delta I \bar{V} + \bar{I} \delta V) \cos(\bar{k} u_i + \bar{\phi}) + \bar{I} \bar{V} \delta k \sin(\bar{k} u_i + \bar{\phi}) u_i + \bar{I} \bar{V} \sin(\bar{k} u_i + \bar{\phi}) \delta \phi \quad (6)$$

Defining

$$D \equiv \begin{pmatrix} 1 & \cos(\bar{k} u_1 + \bar{\phi}) & \sin(\bar{k} u_1 + \bar{\phi}) & \sin(\bar{k} u_1 + \bar{\phi}) u_1 \\ 1 & \cos(\bar{k} u_2 + \bar{\phi}) & \sin(\bar{k} u_2 + \bar{\phi}) & \sin(\bar{k} u_2 + \bar{\phi}) u_2 \\ \vdots & \vdots & \vdots & \vdots \\ 1 & \cos(\bar{k} u_n + \bar{\phi}) & \sin(\bar{k} u_n + \bar{\phi}) & \sin(\bar{k} u_n + \bar{\phi}) u_n \end{pmatrix}$$

and

$$\delta x \equiv \begin{pmatrix} \delta I \\ \bar{V} \delta I + \bar{I} \delta V \\ \bar{I} \bar{V} \delta k \\ \bar{I} \bar{V} \delta \phi \end{pmatrix}$$

we have the relation

$$\delta y = D \delta x. \quad (7)$$

We note that Eq. (7) may be viewed as a linearized model in the neighborhood of the true value of the intensity, visibility, wave number, and phase. Now, suppose  $\delta y^{\text{err}}$  is a random or systematic error in the signal. As a linear approximation, the effect on the calibration parameters  $I, V, k, \phi$  may be found from a least-squares fit of Eq. (7) to  $\delta y^{\text{err}}$  which has the solution

$$\delta x = D^\dagger \delta y^{\text{err}} \quad (8)$$

with  $D^\dagger$  being the pseudoinverse of  $D$ . When there is noise in the  $y_i$ 's, (8) gives the covariance of  $\delta x$

$$\text{Cov}(\delta x) = D^\dagger \text{Cov}(y) (D^\dagger)^T, \quad (9)$$

where  $\text{Cov}(y)$  is the covariance matrix for  $y$ . The definition of  $\delta x$  gives the variance for the wave number and phase as

$$\begin{aligned} \text{Var}(k) &= \frac{1}{\bar{I} \bar{V}} \text{Cov}(\delta x)_{33} = \frac{1}{\bar{I} \bar{V}} D_3^\dagger \text{Cov}(y) (D_3^\dagger)^T, \\ \text{Var}(\phi) &= \frac{1}{\bar{I} \bar{V}} \text{Cov}(\delta x)_{44} = \frac{1}{\bar{I} \bar{V}} D_4^\dagger \text{Cov}(y) (D_4^\dagger)^T, \end{aligned} \quad (10)$$

where  $D_3^\dagger$  and  $D_4^\dagger$  are the 3rd and 4th row vectors of the matrix  $D^\dagger$ . For simplicity, assume that each measurement has independent noise with the same variance,  $\text{Cov}(y) = \sigma_y^2 I$ .

$$\text{Cov}(\delta x) = (D^T D)^{-1} \sigma_y^2, \quad (11)$$

where we have used the expression

$$D^\dagger = (D^T D)^{-1} D^T \quad (12)$$

for the pseudoinverse of  $D$ . It can be shown that for long stroke length (the range of the OPD over which the fringe measurement is performed), with uniform velocity, the so called ‘‘information matrix’’  $D^T D$  is approximately diagonal

$$D^T D \approx \begin{pmatrix} N & 0 & 0 & 0 \\ 0 & \frac{N}{2} & 0 & 0 \\ 0 & 0 & \frac{NL^2}{12} & 0 \\ 0 & 0 & 0 & \frac{N}{2} \end{pmatrix}, \quad (13)$$

where  $N$  is the number of dither steps and  $L$  is the stroke length[5]. Thus the variances of  $k$  and  $\phi$  are simply

$$\text{Var}(k) = \frac{1}{IV} \text{Cov}(\delta x)_{33} = \frac{12\sigma_y^2}{IVNL^2}, \quad \text{Var}(\phi) = \frac{1}{IV} \text{Cov}(\delta x)_{44} = \frac{2\sigma_y^2}{IVN}. \quad (14)$$

We note that the variance of the wave number decreases quadratically as the stroke length increases[4].

## 4 Calibration of the FAM fringe signal on the MAM test bed

In this section, we show the least-squares calibration results from applying the algorithm to the FAM laser interference fringe of the MAM test bed. For a laser source, the monochromatic fringe model is valid. In Fig. 1, we display the fringe signal as function of the delay modulation positions measured by metrology. Applying the least-squares calibration algorithm, we obtain the calibrated wavelength, dispersion phase offset, intensity and visibility shown in Fig. 2. The range of OPD is about  $[-10, 10]\mu m$  corresponding to a stroke length of  $L \approx 20\mu m$ . The number of measurements is  $N = 2201$ . The scan over the OPD range is called one stroke and takes about 5.12 seconds. We used 180 strokes of data in the plots. The fringe signal shown in Fig. 1 is close to a sine fringe. This is consistent with the measured phase, which is approximately 1.85rad. We also used subsets of the data so as to analyze shorter stroke lengths. Using the fact that the FAM laser wavelength is 659.543nm, we display the wavelength calibration error as function of the stroke length in Fig. 3. The result shows that the least-squares algorithm determines the wavelength with error less than 10pm. Because the FAM laser light is generated by doubling the metrology laser, and the metrology laser is used to monitor the OPD during the calibration, this technique is insensitive to laser wavelength drift. It remains sensitive, however, to noise sources such as detection noise. This study

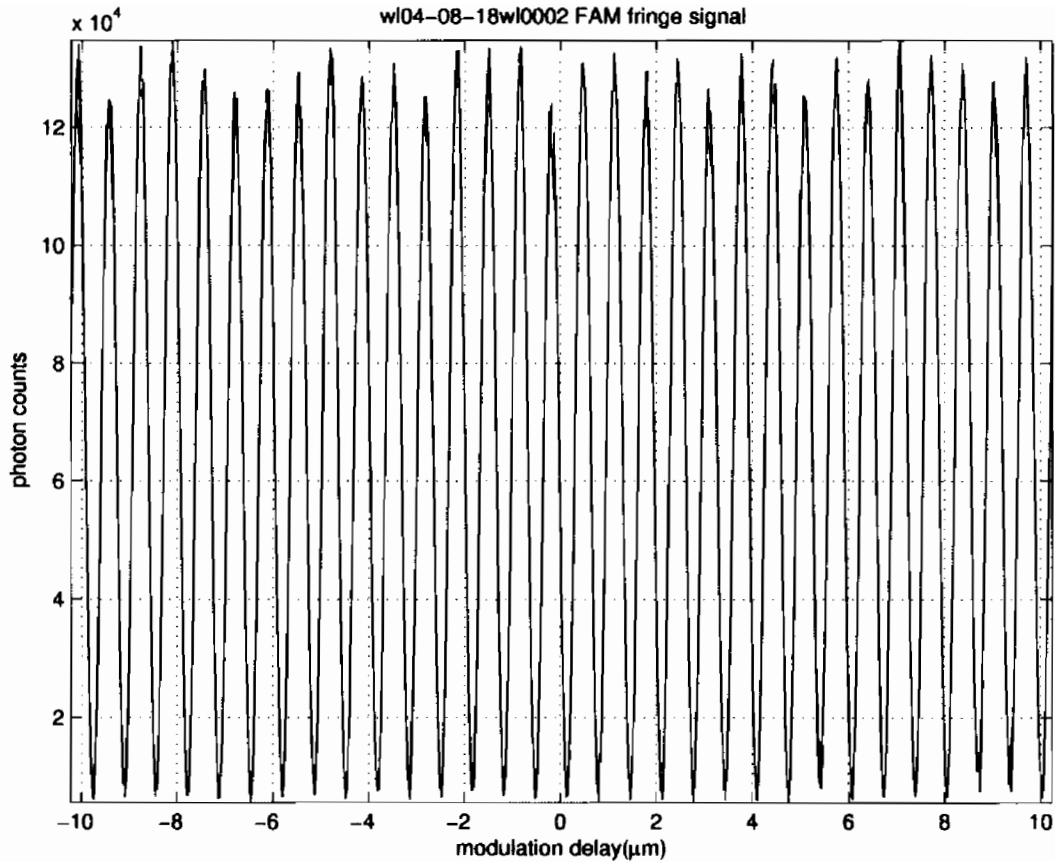


Figure 1: FAM fringe signal as function of the modulated delay

shows that the sensitivity to noise decreases when the stroke length increases. The small bias shown in Fig. 3 is probably due to a small amount of light from the MAM white light source which is also detected by the FAM fringe detector.

## 5 Quasi-monochromatic model and least-squares calibration

So far we have assumed that the fringe signal is developed by interfering monochromatic light. For SIM the light sources are the stars. The non-zero bandwidth of the light source and detector produces a fringe pattern with an envelope that is inversely proportional to the bandwidth. Ignoring the envelope leads to a model error that in turn causes calibration errors. When a long stroke is used, the effect of the envelope becomes even more important. We shall first present a quadratic envelope model derived in Appendix A and then describe a technique for incorporating the envelope effect into the least-squares calibration.

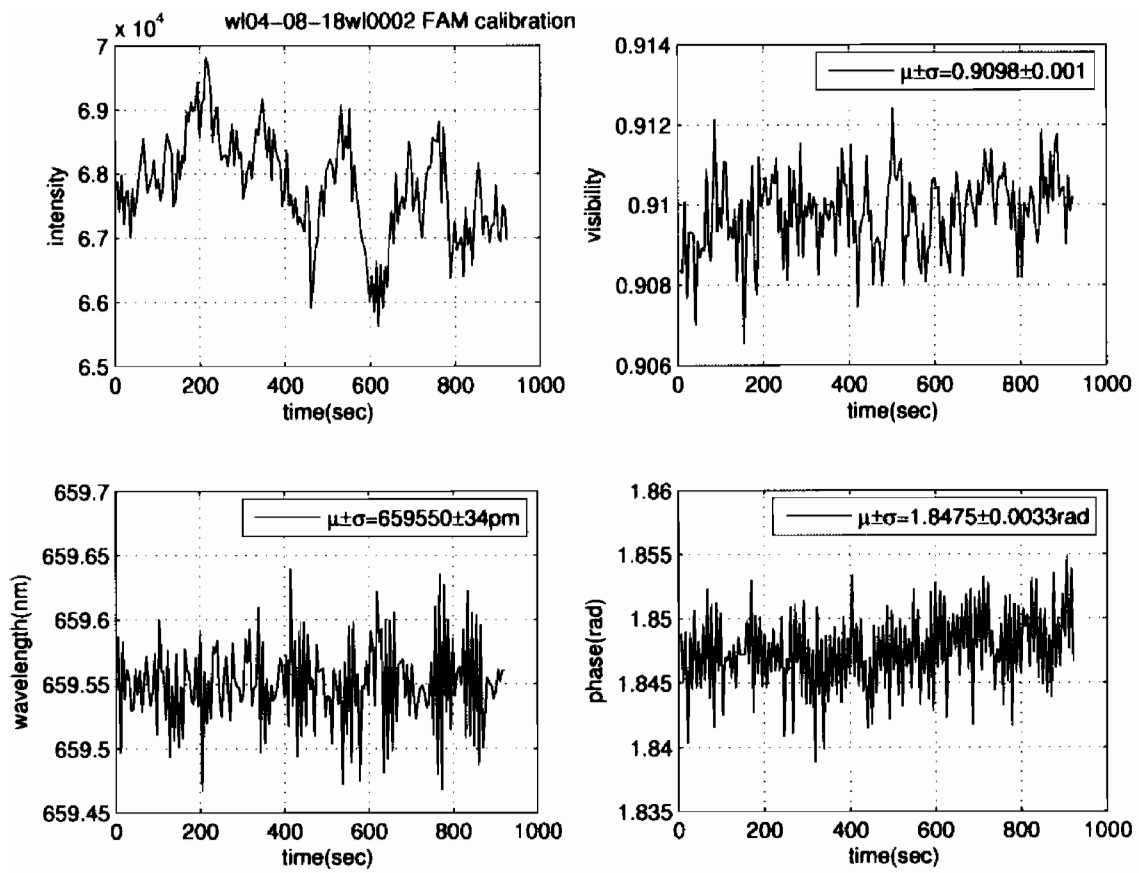


Figure 2: Calibration result of FAM fringe signal using 20  $\mu\text{m}$  stroke length.

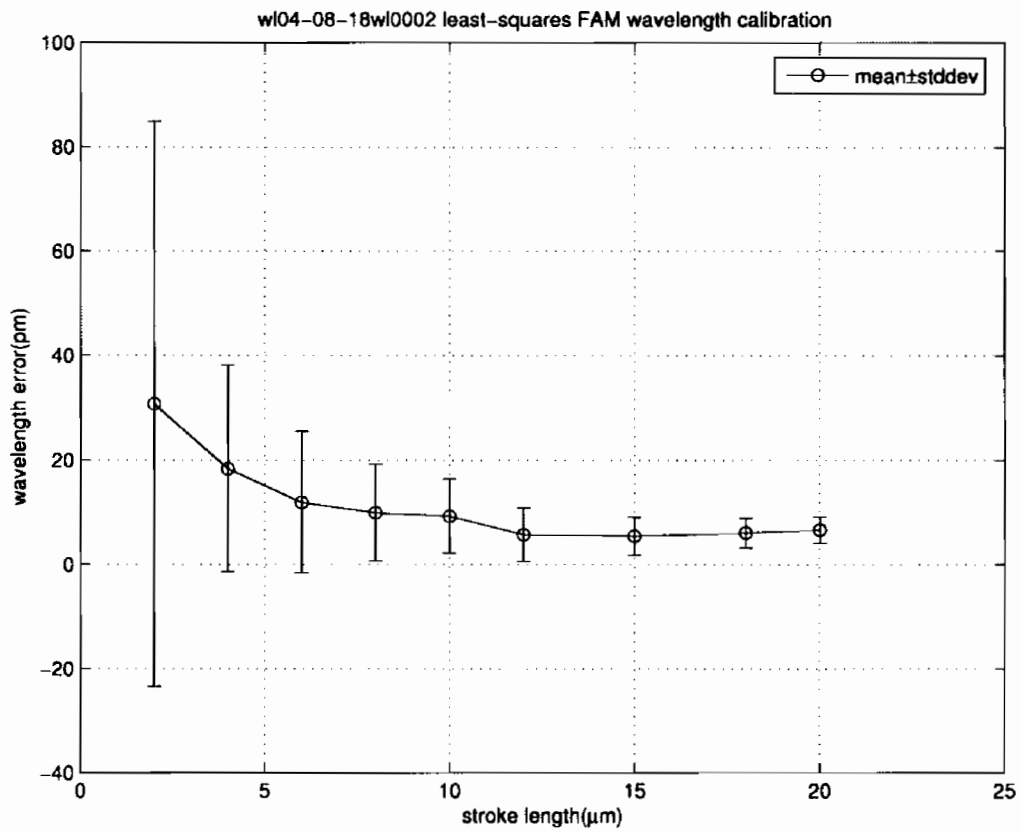


Figure 3: Wavelength calibration error using different stroke length

The generic white light fringe model for a detection bandwidth  $[k_-, k_+]$  is

$$y(u) = \int_{k_-}^{k_+} dk I(k) [1 + V(k) \cos(ku + \phi(k))] \quad (15)$$

where  $y$  is the fringe measurement and  $u$  is the optical path difference;  $I(k)$ ,  $V(k)$ , and  $\phi(k)$  are the spectrum, visibility, and dispersion, respectively. For a narrow bandwidth  $\Delta ku \ll 1$  with  $\Delta k \equiv k_+ - k_-$ , the fringe signal as a function of the optical path difference is expressed as

$$y(u) \approx \bar{I} \left\{ 1 + \bar{V} \left[ 1 - \frac{1}{2} \sigma_k^2 (u + \phi'(\bar{k}))^2 \right] \cos(\bar{k}u + \bar{\phi}) \right\}, \quad (16)$$

where  $\bar{I}$ ,  $\bar{V}$ ,  $\bar{k}$ ,  $\bar{\phi}$  are the effective intensity, visibility, wave number, and dispersion phase for the channel,  $\sigma_k^2$  is the second moment of the spectrum across the bandwidth, and  $\phi'(\bar{k})$  is the group delay evaluated at the effective wave number. (These quantities are all defined in Appendix A.) Qualitatively, the model (16) is a monochromatic signal with a quadratic envelope characterized by the group delay  $\phi'(\bar{k})$  and the second moment  $\sigma_k^2$ , which determine the center and the width of the envelope, respectively. Even for long stroke fringe data, the effect of the envelope factor is small compared to that of the monochromatic factor. Therefore, we treat the fringe envelope portion as a perturbation to the monochromatic signal.

We now turn to a least-squares calibration that incorporates the envelope fringe model. We first consider the least-squares fitting problem with the following model

$$y = A(k)x + \delta y \quad (17)$$

where  $y$  is the fringe measurement and  $\delta y$  is a systematic error of the model. For example,  $y$  is the white light fringe and  $\delta y$  represents the fringe envelope portion as a systematic model error. Our main idea is to “project away”  $\delta y$  using a projection operator  $P$ , *i.e.*  $P\delta y = 0$ . Because  $P$  projects vectors onto the subspace orthogonal to  $\delta y$ , solving the least-squares fitting problem based on the following model

$$Py = PA(k)x \quad (18)$$

effectively removes the systematic error. This technique is adopted in the least-squares calibration algorithm to incorporate the fringe envelope. It should be noted that these gains are not without cost. We lose sensitivity because the projection operator annihilates the observation information in the subspace spanned by  $\delta y$ . In the extreme situation where the subspace spanned by the systematic error  $\delta y$  contains the whole signal space spanned by  $A(k)x$ , this technique does not work at all because the projection  $Py$  annihilates the signal completely. The best situation is, of course, that  $\delta y$  is orthogonal to the signal  $A(k)x$ . Practically, we are almost always in between the two situations. In general there is some reduction in the signal to noise ratio (SNR) due to the projection operator.

To make use of the idea, let  $\delta y$  represent the signal error due to using the monochromatic model (1). Explicitly the fringe envelope portion of the signal is

$$\delta y = -\frac{1}{2}\bar{I}\bar{V}\sigma_k^2(u + \phi'(\bar{k}))^2 \cos(\bar{k}u + \bar{\phi}). \quad (19)$$

It is convenient to define two vectors

$$e_1 \equiv u_i \cos(ku_i + \phi), \quad e_2 \equiv u_i^2 \cos(ku_i + \phi) \quad i = 1, 2, \dots, N. \quad (20)$$

In order to construct a projection operator  $P$  that annihilates  $e_1$  and  $e_2$ , we need to know  $k$  and  $\phi$  in advance. We shall take a perturbation approach. As the first approximation, we shall ignore completely the fringe envelope to get initial estimates for  $k$  and  $\phi$ . With these we can choose  $P$  so that  $Pe_1 = Pe_2 = 0$ . Since we do not know  $k$  and  $\phi$  exactly, the envelope may not be completely annihilated by  $P$ . In general, the wave number is less sensitive to the fringe envelope error [5]. The envelope signal that is not projected away is mainly due to the deviation of the initial estimation of  $\phi$  from its true value. To ensure we project away the envelope signal even when  $\phi$  is not precisely known, we include a third vector  $e_3$  defined

$$e_3 \equiv u_i^2 \sin(ku_i + \phi), \quad (21)$$

as part of the error signal and require  $P$  to satisfy the additional condition  $Pe_3 = 0$ . We do not include the vector  $\sin(\bar{k}u_i + \bar{\phi})u_i$  in this development for two reasons. First of all, in general  $e_1$  is smaller than  $e_2$  for longer strokes where the fringe envelope is more important. Since  $\bar{\phi}$  is already known to first order, the error parallel to the vector  $\sin(\bar{k}u_i + \bar{\phi})u_i$  is very small. Secondly, the signal parallel to  $\sin(\bar{k}u_i + \bar{\phi})u_i$  should not be projected away because our main signal is  $\cos(\bar{k}u_i + \bar{\phi})$  and we are looking for the best  $\bar{k}$ ,  $\bar{\phi}$  to fit this signal. The variation of  $\bar{k}$  generates a change in the signal parallel to  $\sin(\bar{k}u_i + \bar{\phi})u_i$ . Thus if we work in a subspace orthogonal to this vector, we would not be able to determine  $\bar{k}$  because its variation generates a zero component in the subspace where the fitting is being done. This is an example of projecting away the essential signals as discussed at the end of the last section.

Treating  $e_1$ ,  $e_2$ , and  $e_3$  as column vectors, the QR-factorization

$$QR = [e_1 e_2 e_3] \quad (22)$$

yields the matrix  $Q$  with column vectors forming a set of basis vectors for the fringe envelope signal subspace. The projection  $P$  onto the orthogonal complement is then

$$P = 1 - QQ^T. \quad (23)$$

With  $P$ , in principle, we can simply replace the  $A(k)$  matrix in the monochromatic case by  $PA(k)$  to project away the fringe model error corresponding to the envelope. However, since we already have an initial estimate of  $k$ ,  $\phi$ ,  $I$ , and  $V$ , and because the

envelope is a perturbation to the main signal, we expect that these initial estimates are in the neighborhood of the true effective wave number, phase, intensity, and visibility, respectively. Therefore, it is convenient to use the linearized model (7) to determine the correction to the initial estimates. Therefore, we shall solve for  $\delta x$  with

$$P\delta y = PD\delta x, \quad (24)$$

where  $\delta y$  is the residual signal after subtracting the monochromatic signal portion with the initial estimated parameters.

As we mentioned previously, it is very important to do a sensitivity analysis to see whether we lose essential signals after applying the projection operator  $P$ . The signals that are crucial in determining the calibration parameters are the signals sensitive to the signal parameter variation. In view of Eq. (7), the variation in the signal as a response to variation of the model parameters can be expressed as  $\delta y = D\delta x$ . For a reasonable dither step vector,  $D$  is a full rank matrix so that the least-squares calibration algorithm is adequate to determine the model parameters. The sensitivity may be mainly captured by the ‘‘information matrix’’  $D^T D$  as this is related to the variance of  $\delta x$  when the covariance matrix of  $y$  is proportional to an identity matrix. With the projection, the new sensitivity Eq. 24 leads to the new ‘‘information matrix’’  $D^T P D$ . As shown in reference [5] that for long stroke data or when  $N \gg 1$ ,  $P D$  is still a full rank matrix. Similar to  $D^T D$  shown in Eq. (13),  $D^T P D$  is also approximately diagonal with the first and third diagonal values about the same as  $D^T D$  and the second and fourth diagonal values reduced by a factor of 4/9. This means that the visibility and the wave number lose 1/3 sensitivity due to projecting away the envelope.

## 6 Application of Envelope Projection Method to Simulated Fringes

In this section we show results from applying the envelope projection method to a simulated fringe signal over an optical path delay range of  $[-10, 10]\mu m$  for a passband of  $[845, 870]nm$  using the spectrum of a typical M3 star. A dispersion phase equivalent to an extra  $100\mu m$  thick fused silica glass has been included. The visibility is simply chosen to be unity.

We analyze the simulated fringe data using the technique in the previous section. The effectiveness of the envelope projection technique is shown by the results displayed in Fig. 4, Fig. 5, Fig. 6, and Fig. 7. Without including the fringe envelope in the model the errors in phase calibration are on the order of tens of pico meters and the visibility error can be more than 5% for long stroke lengths. The effectiveness of the technique is clearly seen by the reduced stroke length dependency in all the figures displayed. The error in the estimated wave number and intensity are relatively small. For the purpose of comparison we also display the calibration

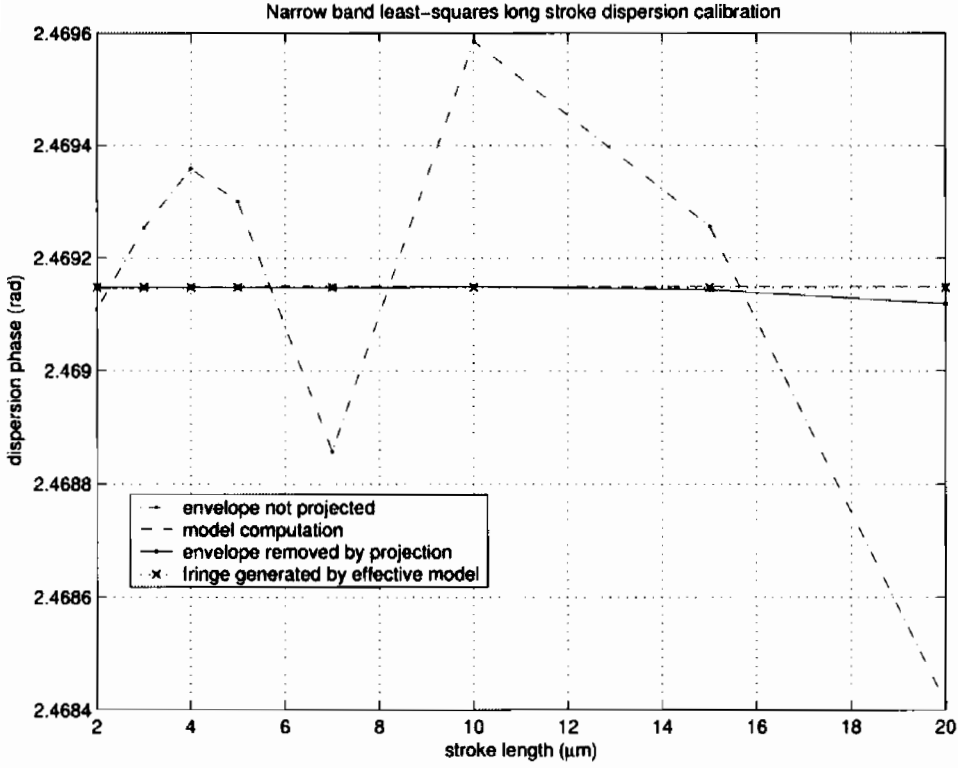


Figure 4: After applying the fringe projection technique, the calibrated results are very close to the results computed by using the effective model. The deviation at long stroke lengths is due to the inadequacy of the quadratic fringe envelope model at large group delays.

results for fringes modeled by the quadratic effective model (16). Note that the deviation from the effective model parameters for very long stroke length are due to fringe envelope effects that are higher than second order because the calibration results for a fringe that is modeled by only the quadratic effective model does not show these deviations.

## 7 Fringe Envelope Shape Estimation

In this section, we show how to estimate the fringe envelope shape based on our model (16). The fringe envelope shape is parameterized by its width and center as shown in the model which is described by  $\sigma_{\bar{k}}^2$  and  $\phi'(\bar{k})$ . The task is to estimate them using the fringe signal  $y_i$ . After finding  $\bar{k}$  and  $\bar{\phi}$  with the projection method, the fringe model (16) may be written as

$$y_i = c_1 + c_2 \cos(ku_i + \phi) + c_3 u_i \cos(ku_i + \phi) + c_4 u_i^2 \cos(ku_i + \phi), \quad (25)$$

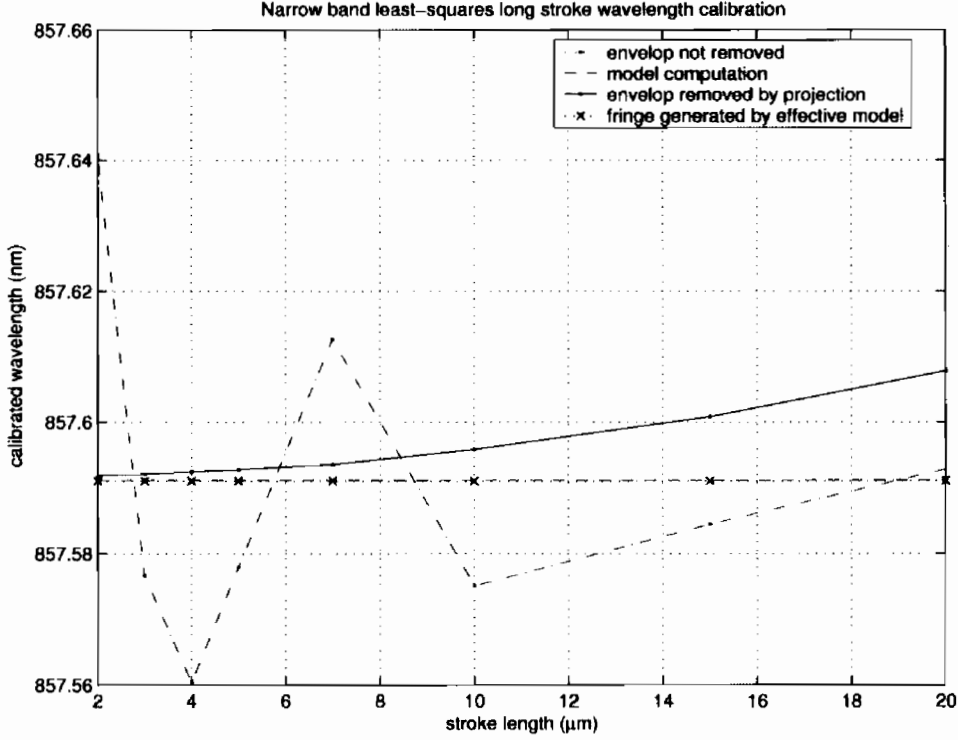


Figure 5: After applying the fringe projection technique, the calibrated results are very close to the results computed by using the effective model.

where  $c_i$ ,  $i = 1, 2, 3, 4$  are parameters related to the effective model parameters in the following way

$$c_1 = \bar{I}, c_2 = \bar{I}\bar{V} \left( 1 - \frac{1}{2}\sigma_{\bar{k}}^2\phi'(\bar{k})^2 \right), c_4 = -\bar{I}\bar{V}\sigma_{\bar{k}}^2/2, c_3 = 2c_4\phi'(\bar{k}). \quad (26)$$

The inverse relations are

$$\bar{I} = c_1, \bar{V} = (c_2 + c_3^2/(4c_4))/c_1, \phi'(\bar{k}) = c_3/(2c_4), \sigma_{\bar{k}}^2 = -2c_4/(\bar{I}\bar{V}). \quad (27)$$

A least-squares fitting of  $y_i$  to the model (25) provides estimates of  $c_i$ ,  $i = 1, 2, 3, 4$  and thus the estimation of the fringe envelope shape via relationship (27). We note here that with the fringe shape estimation, we may use the the second formula in relation (27) to get a better estimation of the visibility than in Section 5, where the contribution due to  $c_3$  has been ignored. The blue solid line in Fig. 6 displays the visibility calibration result including this improvement.

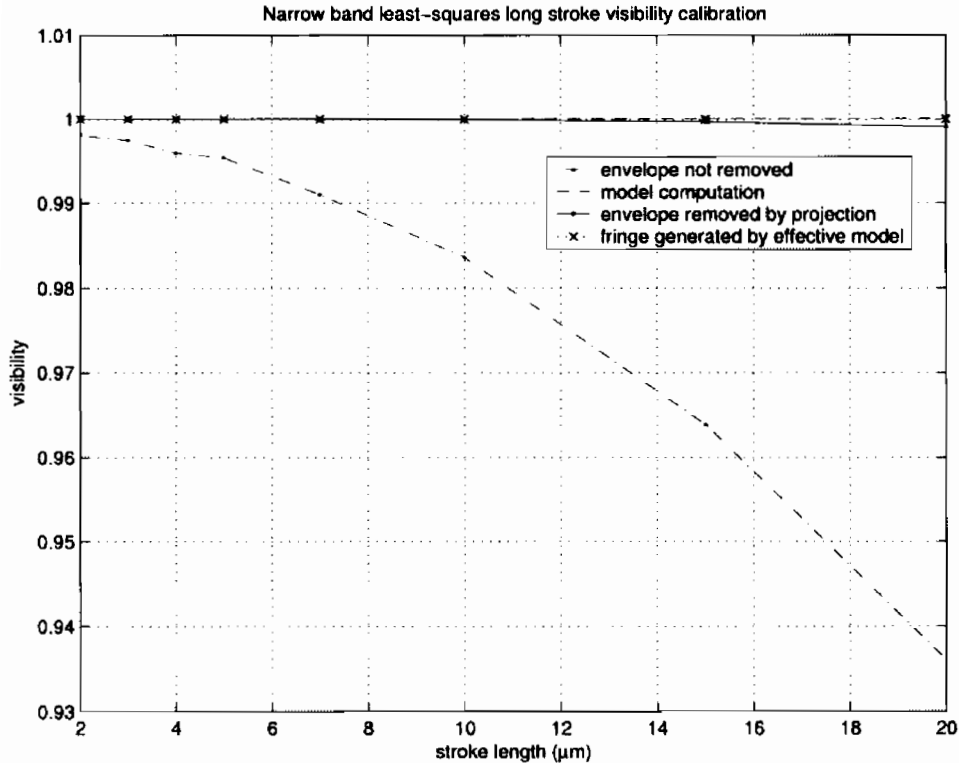


Figure 6: After applying the fringe projection technique, the calibrated visibilities are very close to the results computed by using the effective model. Note that this plot was generated after the improvement discussed in Section 7.

## 8 Application to MAM test bed data

In this section we show the results from applying the calibration algorithm presented in the previous sections to MAM testbed data. Figure 8 shows the fringe for an individual MAM pixel corresponding to a wavelength of approximately 800nm. The fringe envelope effect is evident in this figure even though the CCD pixel detection passband is quite small (10nm between the pixel centers, but due to diffraction effects, the effective pixel width is estimated to be about 25nm). We now show the results of the calibration respectively for the intensity, visibility, wave number, and dispersion with and without taking the fringe envelope into account. Ignoring the envelope effect, the visibility calibration shows a clear decreasing trend, as expected. But even after the projection algorithm is applied there is still a residual trend. This is possibly due to the fact that the quadratic fringe envelope model needs to be augmented with higher order terms to attain sufficient fidelity. Nevertheless, the stroke length dependency is clearly less significant when the projection algorithm is applied.

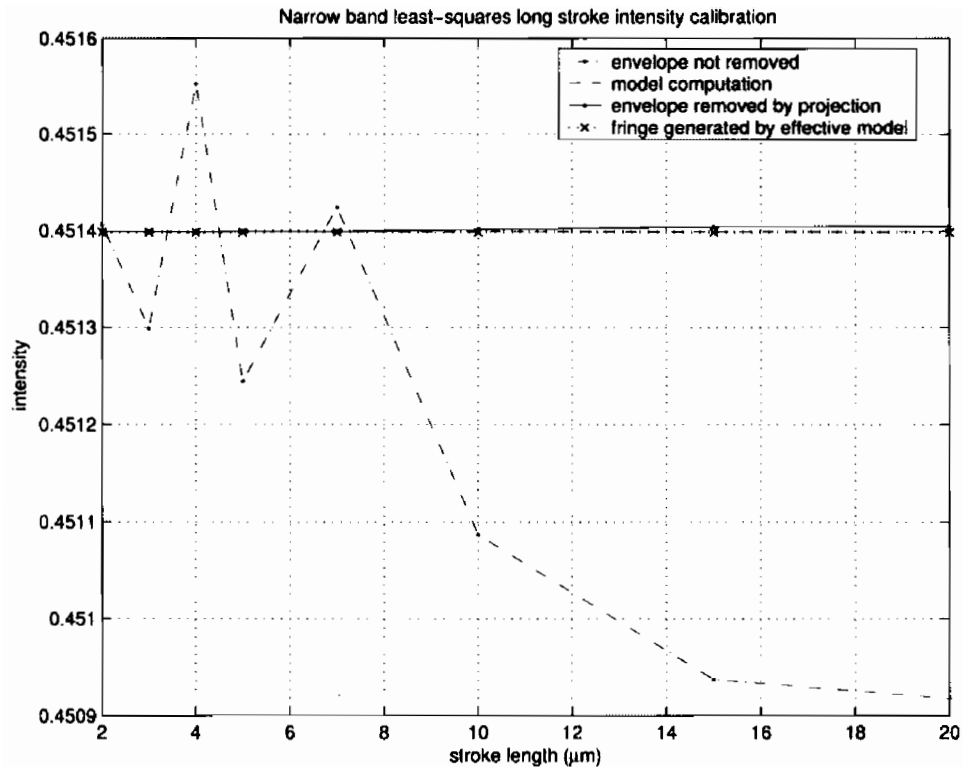


Figure 7: After applying the fringe projection technique, the calibrated results are very close to the results computed by using the effective model.

## 9 Summary

In summary we have presented a least-squares approach to calibrating the fringe model parameters for both monochromatic and narrow band white light fringe signals. The efficacy of the algorithms have been demonstrated on both simulated and experimental data. Experimental agreement of calibrated wavelength to a 10pm accuracy was achieved for laser light. Numerical experiments validated the superiority and necessity of the fringe envelope projection method for calibrating the parameters of narrow band sources. MAM testbed results corroborated these numerical experiments.

## 10 Acknowledgment

This work was prepared at the Jet Propulsion Laboratory, California Institute of Technology, under a contract with the National Aeronautics and Space Administration.

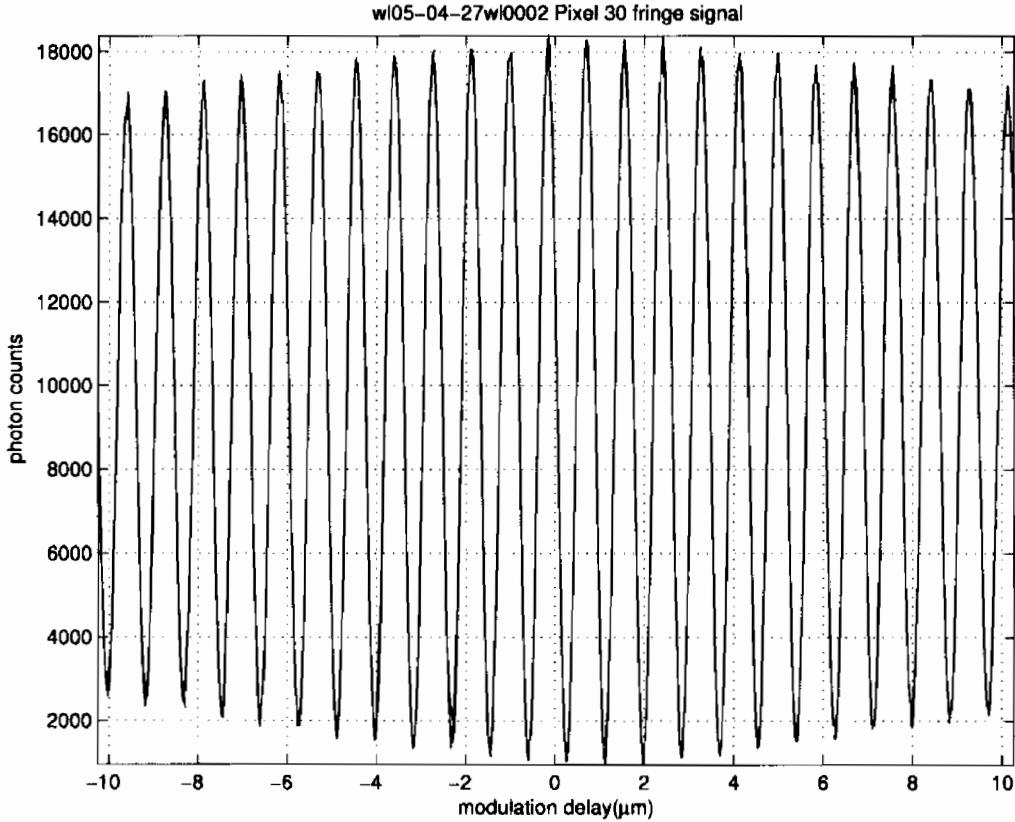


Figure 8: Fringe signal detected by MAM CCD Pixel 30.

## A Quasi-monochromatic fringe model

In this appendix, we derive the quasi-monochromatic model for a narrow band signal. Recall that the generic fringe formula for detection bandwidth  $[k_-, k_+]$  is

$$y(u) = \int_{k_-}^{k_+} dk I(k) [1 + V(k) \cos(ku + \phi(k))] \quad (28)$$

where  $y$  is the fringe measurement and  $u$  is the optical path delay;  $I(k)$ ,  $V(k)$ , and  $\phi(k)$  are the spectrum, visibility, and dispersion function respectively. For a narrow bandwidth  $\Delta ku \ll 1$ , we may make a narrow band expansion about some effective wave number  $\bar{k}$  and phase  $\bar{\phi}$  to be determined in a moment. Assuming that the variation of the dispersion function  $\phi(k)$  over  $[k_-, k_+]$  is small, we can expand the exponential and derive

$$\begin{aligned} y(u) &= \int_{k_-}^{k_+} dk I(k) + \text{Re} \left[ e^{i\bar{k}u + i\bar{\phi}} \int_{k_-}^{k_+} dk I(k) V(k) e^{i((k-\bar{k})u + \phi(k) - \bar{\phi})} \right] \\ &= \bar{I} + \text{Re} \left\{ e^{i\bar{k}u + i\bar{\phi}} \int_{k_-}^{k_+} dk I(k) V(k) [1 + i((k-\bar{k})u + \phi(k) - \bar{\phi})] \right\} \end{aligned}$$

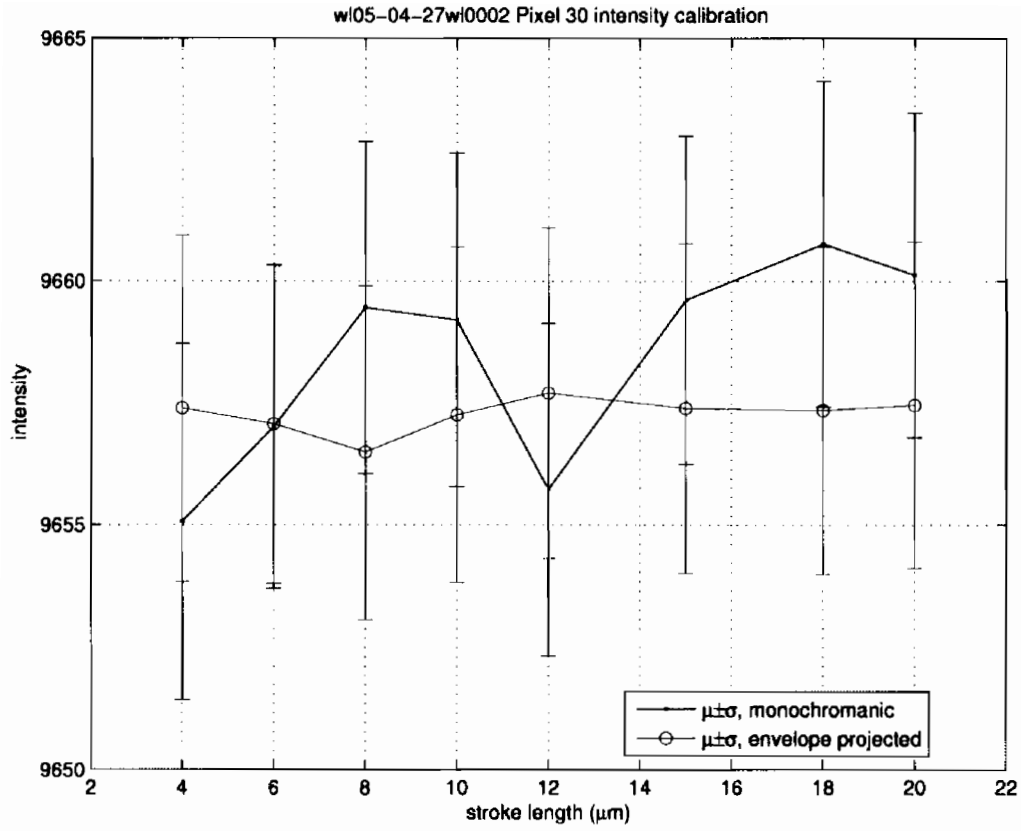


Figure 9: Intensity calibration for pixel 30, the stroke length dependency

$$-\frac{1}{2} \left( (k-\bar{k})u + \phi(k) - \bar{\phi} \right)^2 + O(\Delta k, \delta\phi)^3 \Big\} , \quad (29)$$

where we have defined an effective intensity

$$\bar{I} \equiv \int_{k_-}^{k_+} dk I(k) , \quad (30)$$

and used  $\delta\phi$  to represent the variation of dispersion function  $\phi$  about an effective value  $\bar{\phi}$ . It is natural to define  $\bar{k}$  and  $\bar{\phi}$  as the following

$$\bar{k} \equiv \int_{k_-}^{k_+} dk I(k) V(k) k / \int_{k_-}^{k_+} dk I(k) V(k) , \quad (31)$$

$$\bar{\phi} \equiv \int_{k_-}^{k_+} dk I(k) V(k) \phi(k) / \int_{k_-}^{k_+} dk I(k) V(k) \quad (32)$$

so that the leading order terms in expression (29) vanishes. With these, through the second order, we have

$$y(u) = \bar{I} + \cos(\bar{k}u + \bar{\phi}) \int_{k_-}^{k_+} dk I(k) V(k) \left[ 1 - \frac{1}{2} \left( (k-\bar{k})u + \phi(k) - \bar{\phi} \right)^2 + O(\Delta k, \delta\phi)^3 \right]$$

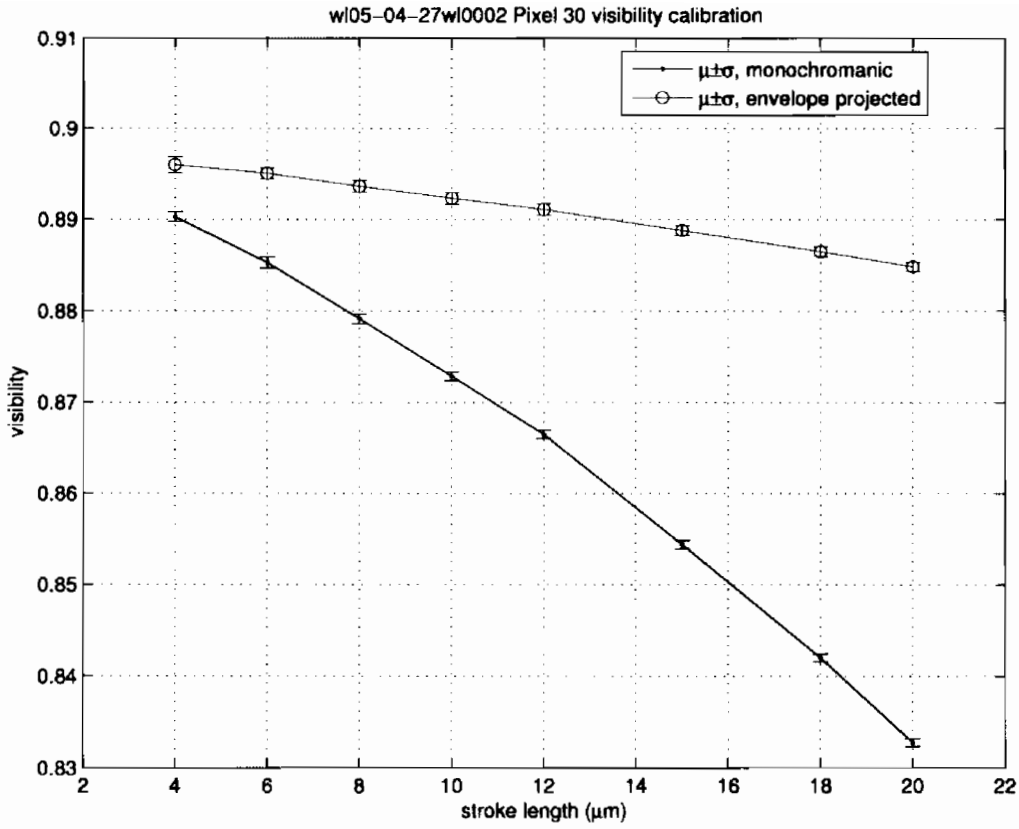


Figure 10: Visibility calibration for pixel 30, the stroke length dependency

$$\approx \bar{I} \left\{ 1 + \bar{V} \left[ 1 - \frac{1}{2} \left( \sigma_k^2 u^2 + 2\sigma_{k\phi} u + \sigma_\phi^2 \right) \right] \cos(\bar{k}u + \bar{\phi}) \right\}, \quad (33)$$

where we have defined

$$\bar{V} = \int_{k_-}^{k_+} dk I(k) V(k) / \bar{I}, \quad (34)$$

$$\sigma_k^2 = \int_{k_-}^{k_+} dk I(k) V(k) (k - \bar{k})^2 / (\bar{I} \bar{V}), \quad (35)$$

$$\sigma_{k\phi} = \int_{k_-}^{k_+} dk I(k) V(k) (k - \bar{k}) (\phi(k) - \bar{\phi}) / (\bar{I} \bar{V}),$$

$$\sigma_\phi^2 = \int_{k_-}^{k_+} dk I(k) V(k) (\phi(k) - \bar{\phi})^2 / (\bar{I} \bar{V}). \quad (36)$$

Eq. (33) is our general quadratic envelope model for narrow band white light fringe. When the dispersion function  $\phi(k)$  is smooth, the following expansion is valid

$$\phi(k) = \phi(\bar{k}) + \phi'(\bar{k})(k - \bar{k}) + \frac{1}{2} \phi''(\bar{k})(k - \bar{k})^2 + O((k - \bar{k})^3), \quad (37)$$

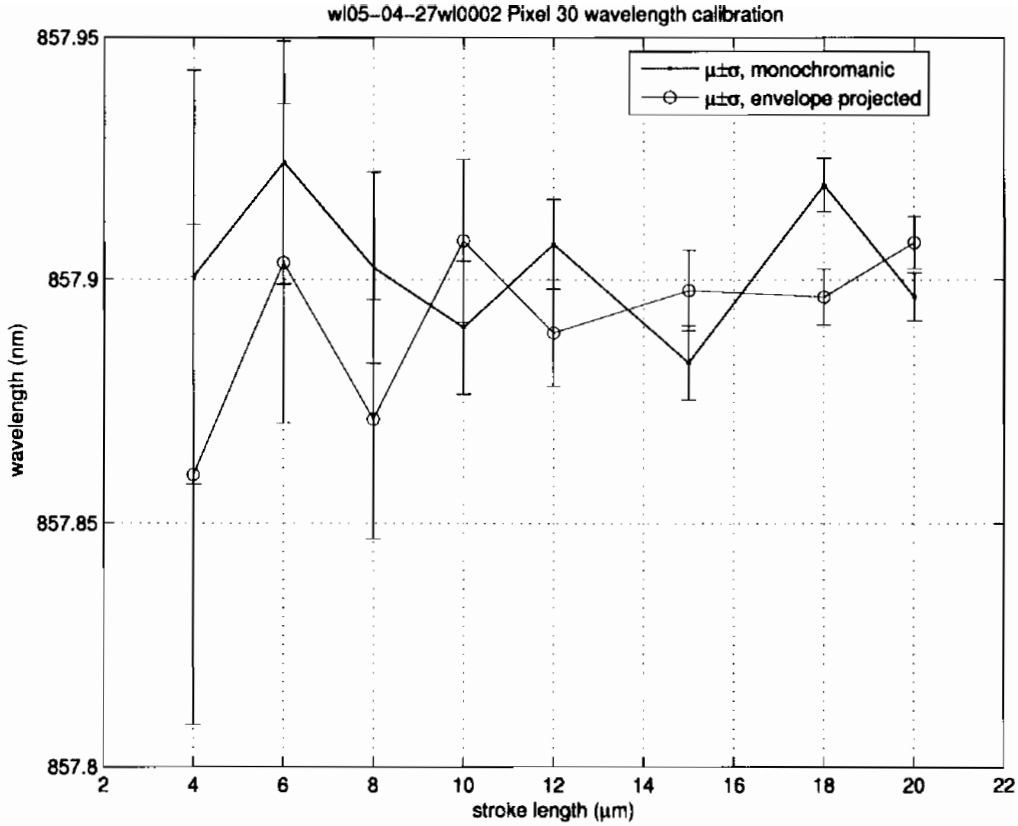


Figure 11: Wavelength calibration for pixel 30, the stroke length dependency

The generic quadratic fringe model (33) may be simplified as

$$y(u) \approx \bar{I} \left\{ 1 + \bar{V} \left[ 1 - \frac{1}{2} \sigma_k^2 (u + \phi'(\bar{k}))^2 \right] \cos(\bar{k}u + \bar{\phi}) \right\}, \quad (38)$$

with the clear physical meaning for  $\phi(\bar{k})$  being the group delay offset from the fringe center. The width of the envelope is determined by the value of the second moment of the wave number  $\sigma_k^2$ . Eq. (38) is the same as the model (16) in section 5.

## References

- [1] *SIM error budget*, a SIM memo.
- [2] Mark Milman, *A narrow angle algorithm, Part 1: Model, algorithm and initial sensitivities.*, a SIM memo.
- [3] J. E. Greivenkamp, "Generalized data reduction for heterodyne interferometry," *Optical Engineering* **23**, 350-352 (1984)

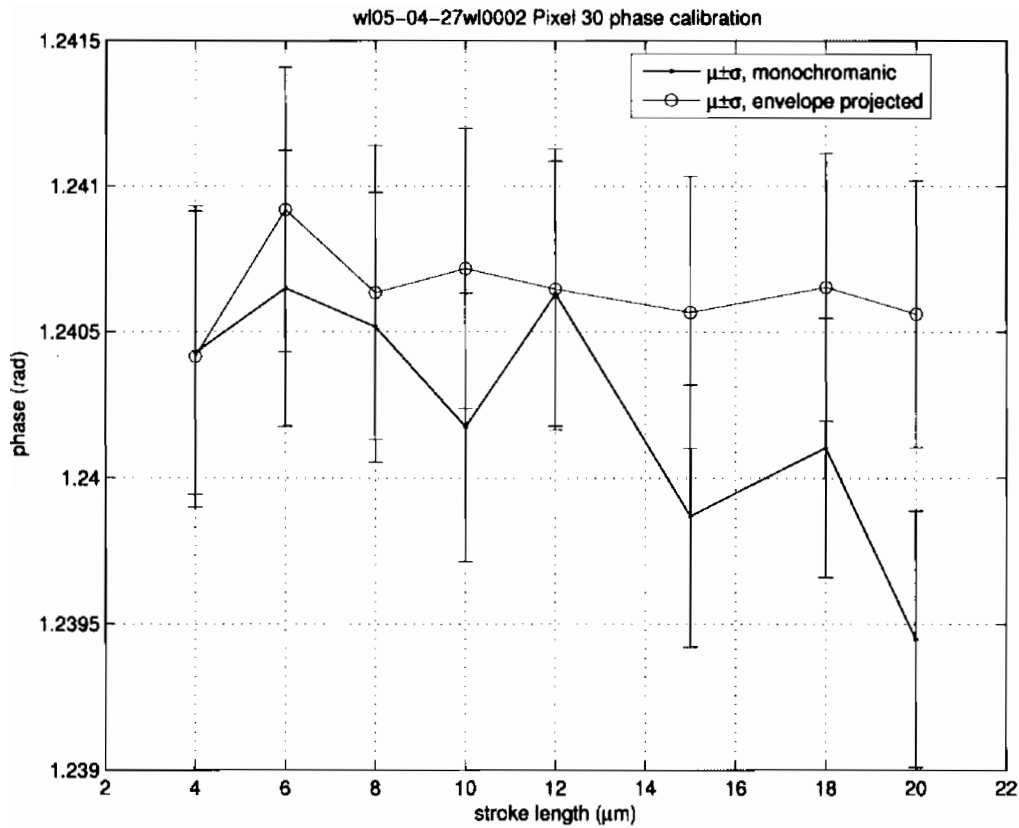


Figure 12: Phase calibration for pixel 30, the stroke length dependency

- [4] M. Milman and J. Shen, *A “short” stroke spectral calibration algorithm; preliminaries*, a SIM Memo.
- [5] Chengxing Zhai, *Fringe Envelope Effect in Least-Squares Calibration and Phase Estimation*, a SIM Memo.